Fully coherent hard X-ray generation by two-stage phase-merging enhanced harmonic generation*

Guang-Lei Wang(王光磊)[1] Wei-Qing Zhang(张未卿)[1] Xue-Ming Yang(杨学明)[1]
Chao Feng(冯超)[2] Hai-Xiao Deng(邓海啸)[2;1]

[1] State Key Laboratory of Molecular Reaction Dynamics, Dalian Institute of Chemical Physics, Chinese Academy of Sciences, Dalian 116023, China
[2] Shanghai Institute of Applied Physics, Chinese Academy of Sciences, Shanghai 201800, China

Abstract: Cascading stages of seeded free electron lasers (FELs) is a promising way to produce fully coherent X-ray radiation. We study a new approach to produce coherent hard X-rays by cascading the recently proposed phase-merging enhanced harmonic generation (PEHG) The scheme consists of one dogleg and two PEHG configurations, and may be one of the leading candidates for the extracted undulator branch in future X-ray FEL facilities. FEL physics studies show that such a scheme is feasible within the present technology and can provide high brightness X-ray radiation pulses with narrow bandwidth and full coherence The radiated peak power at 1 Å wavelength converted from an initial 200 nm seed laser is over 2 GW

Keywords: free electron laser, cascaded PEHG, dogleg, hard X-ray, TGU

PACS: 29.27.Fh, 41.60.Cr, 41.85.Ja **DOI:** 10.1088/1674-1137/40/9/098101

1 Introduction

The hard X-ray free electron laser (FEL) era was reached by the successful lasing of self-amplified spontaneous emission (SASE) [1]. However, because the FEL radiation starts from the initial shot noise, the output of SASE typically has poor longitudinal coherence and large shot-to-shot fluctuations. At the same time, as the most promising way for delivering fully coherent FEL radiation pulses in the ultraviolet and even soft X-ray regions, seeded FEL schemes are being developed worldwide. The world's first seeded FEL user facility, FERMI, started to deliver extreme ultraviolet pulses to users in 2011 [2], and several other FEL facilities based on seeded configurations are under construction or consideration [3–5].

Generally, in a seeded FEL configuration like high-gain harmonic generation (HGHG), an external coherent seed laser pulse is employed to interact with the electron beam in a short undulator (modulator) to generate sufficient beam energy modulation. The electron beam is then sent through a magnetic chicane (dispersion section) where the energy modulation is converted into density modulation and micro-bunching on the scale of the optical seed laser wavelength is established. Taking advantage of the Fourier transform of the density modulation containing abundant components at high harmonics of the seed, a coherent short-wavelength signal that dominates over the beam shot noise can be amplified by a relatively long undulator (radiator) resonant at the harmonic of interest of the seed. As expected from theory, the success of seeding schemes such as HGHG [6–9] and echo-enabled harmonic generation (EEHG) [10–13] lead to the possibility of generating short wavelength radiation pulses with high brilliance and excellent longitudinal coherence.

It is expected that, more scientific opportunities, ranging from materials and biomaterials sciences, nanosciences, plasma physics, molecular physics and chemistry, will emerge as fully coherent X-ray FEL sources are exploited. However, currently single-stage seeded FELs are not capable of reaching the hard X-ray region, because of limited frequency up-conversion efficiency [14]. Therefore, cascading stages of HGHG and EEHG have been proposed to produce fully coherent X-ray radiation [15–16]. More recently, a novel seeded FEL scheme, so-called phase-merging enhanced harmonic generation (PEHG) [17–18], has been proposed to generate fully coherent short-wavelength radiation. In PEHG, when the transversely dispersed electrons pass through a transverse gradient undulator (TGU) modulator [19], around the zero-crossing of the seed laser, electrons of

Received 24 February 2016, Revised 29 April 2016
* Supported by the National Natural Science Foundation of China (21127902 & 11322550) and Ten Thousand Talent Program
1) E-mail: denghaixiao@sinap.ac.cn

the same kinetic energy will merge into the same longitudinal phase due to the transverse-longitudinal coupling, which enables a supreme frequency up-conversion efficiency with a very small energy modulation. Theoretical calculations and numerical simulations indicate that a single-stage PEHG is capable of generating high power soft X-ray radiation with a narrow bandwidth close to Fourier-transform-limited. Moreover, it is found that PEHG has almost no response to the beam energy curvatures produced in the acceleration process [20].

These above-mentioned properties make PEHG a promising candidate for short-wavelength FELs. Meanwhile, more and more extracted undulator branches are considered in modern X-ray FEL user facilities, e.g., in SACLA, PAL-XFEL and Swiss-FEL [21–23], which offer an opportunity of large transverse dispersion for a PEHG operation. Under such circumstances, cascading stages of PEHG with the "fresh bunch" technique [24] is a straightforward idea for extending to the hard X-ray region. In this paper, we first describe the principle of the cascaded PEHG. Then detailed considerations of the hard X-ray generation by PEHG schemes are shown. The main issues, including the design of the dispersion dogleg, undulator system and the seed laser system, are presented.

2 Layout of cascading PEHG

The PEHG scheme combines a dispersion dogleg and a TGU modulator, which induce a transverse-longitudinal phase space coupling. Firstly, the e-beam is transversely dispersed by the dogleg, then the transversely dispersed electrons pass through the TGU modulator with transverse gradient α, and dimensionless undulator parameter K. Around the zero-crossing of the seed laser, electrons with the same energy will merge into the same longitudinal phase. PEHG holds great promise for generating fully coherent short-wavelength radiation due to the advantage of the phase merging effect, the soft X-ray wavelength range can be reached in a single stage PEHG.

Even although the PEHG scheme has a supreme up-conversion efficiency, it is still difficult to achieve 1 Å FEL radiation from a commercially available seed laser. Motivated and stimulated by the recent and great success of two-stage HGHG demonstrations and operations at SDUV-FEL [25–27] and FERMI [28], a straightforward and promising idea is the multi-stage PEHG scheme. Now, we investigate the possibility of producing hard X-rays using a cascaded PEHG scheme. The layout is shown in Fig. 1, and consists of a PEHG, a magnetic delay chicane and an HGHG configuration. The HGHG part is equivalent to a second PEHG by jointly using the transverse dispersion section in the initial stage.

In Fig. 1, the dogleg is utilized to obtain a transverse dispersion in the whole e-beam, then a short seed laser pulse is injected and adjusted in the first TGU modulator (M1). To make sure only the e-beam energy of the tail part is modulated, this e-beam is sent through the dispersion section (DS1), which converts the energy modulation into a density bunching. Meanwhile the head part, called the "fresh" part hereafter, also experiences the same process as the tail part in the first stage, in the absence of energy modulation. Then the FEL radiation from the first stage radiator (R1), which uses the e-beam tail part, serves as the seed laser of the second stage. The magnetic chicane between the two stages is used to realize the "fresh bunch" delay and make sure the e-beam can exactly interact with the seed laser in the second stage modulator. Because the fresh part has already been transverse dispersed by the dogleg, the second stage together with the dogleg can also be considered as a whole PEHG. In the second stage PEHG, considering the stringent beam requirements and practical operation difficulties at short wavelengths, a normal modulator (M2) and a TGU (M3) is used for the energy modulation and the transverse manipulation of the electron beam, respectively. It has been theoretically demonstrated that such a configuration has a larger efficiency of density modulation and is much more flexible for practical operation [18]. In this configuration, the output from the second radiator (R2), which is tuned at the harmonic of the first radiation, can be extended to even the hard X-ray region. In addition, the radiator of the first stage can work at the coherent harmonic generation (CHG) [29–30] or saturation regime, depending on the required seed laser power for the second stage.

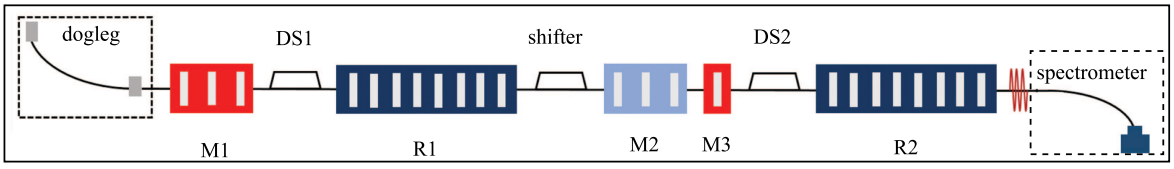

Fig. 1. Schematic layout of cascaded PEHG to produce hard X-rays.

3 Theoretical optimization of cascaded PEHG

If one takes the transverse effects into accounts, the PEHG bunching can be written as:

$$b = J_h(hD\Delta\gamma_s)\exp\left(\frac{h^2D\sigma_x^2}{2\eta^2}\right), \quad (1)$$

where h is the harmonic number, $D = k_sR_{56}/\gamma$, k_s is the wave number of the seed laser, R_{56} is the strength of the dispersive chicane, γ is the electron beam Lorentz factor, $\Delta\gamma_s$ is the energy modulation induced by seed laser, J_h is the $h^{\rm th}$ order Bessel function, η is the transverse dispersion of the dogleg and σ_x is the transverse beam size. The bunching of PEHG is the same as the standard HGHG with an equivalent energy spread of $\sigma_{\rm eff} = \sigma_x/\eta$ [18].

The optimal relationship between the dogleg and the design parameters of TGU is

$$TD = -B, \quad (2)$$

where $T = \dfrac{k_sL_{\rm m}K_0^2\alpha\sigma_x}{2\gamma^2}$ is the dimensionless gradient parameter of a TGU with α and K_0 representing the transverse gradient and central dimensionless parameter respectively. The reasonable beam size in the TGU modulator is $\sigma_x = \sqrt{\varepsilon_xL_{\rm m}/2\gamma}$, with ε_x and $L_{\rm m}$ for the normalized horizontal emittance and the modulator length, respectively.

According to Eq. (2), the optimized condition of α and η can be summarized in Eq. (3),

$$\eta = -\frac{2\gamma(h+0.81h^{1/3})}{\alpha hk_sL_{\rm m}K_0^2\sigma_r}, \quad (3)$$

where A is the energy modulation amplitude induced by seed laser and σ_r is the RMS beam energy spread.

To explore the performance of a cascaded PEHG with realistic parameters, we suppose a hard X-ray FEL, using a group of parameters close to the Swiss-FEL: a 6 GeV electron beam with sliced energy spread of 0.6 MeV, i.e., a relative energy spread of 1×10^{-4}, normalized emittance of 1.0 μm·rad, and peak current of 3 kA is expected at the exit of the LINAC for efficient FEL lasing. In the FEL section, 1 Å FEL radiation is generated as the $2000^{\rm th}$ harmonic of the initial seed laser.

Now presenting the details, we consider a dogleg with η = 1.4 m for effective transverse dispersion of the e-beam. A 200 nm seed laser is then imported. The peak power is about 4 GW for sufficient energy modulation. The FEL radiation in each stage will inherit the properties of this high quality fundamental seed laser, and results in a Fourier transform limited FEL radiation pulse. After the two-stage cascaded process, 1 Å FEL radiation is amplified to saturation with a peak power beyond 2 GW by the 40 m long radiator. The parameters for the undulator, dogleg, and seed laser system are summarized in Table 1.

Table 1. The main parameters of the hard X-ray FEL facility.

	the first stage		the second stage		
undulator	M1	R1	M2	M3	R2
undulator period	0.2 m	0.04 m	0.04 m	0.04 m	0.015 m
undulator length	2 m	25 m	2 m	0.4 m	40 m
laser wavelength	200 nm	4 nm	4 nm		0.1 nm
laser power	4 GW	10 GW	10 GW		2 GW
laser size	100 μm	50 μm	100 μm		50 μm
laser pulse length	50 fs	50 fs	50 fs		50 fs
dispersion R56	0.105 mm			1.5 μm	

For the case of $A = 5$, according to Eq. (1), the PEHG bunching factor at different harmonics is plotted in Fig. 2(a). Due to the equivalent energy spread compression, the theoretical maximum value at the $50^{\rm th}$ harmonic is about 18%. Three-dimensional simulation is utilized to illustrate the phase space evolution in the PEHG scheme, and the longitudinal phase space after passing through DS1 is shown in Fig. 2(b). The initial beam energy spread is artificially rearranged and suppressed in the PEHG scheme by the so-called phase-merging effect. The energy spread compression factor $C = \eta\sigma_r/\gamma\sigma_x$ is about 5 and this compression makes the available harmonic number increase about 5 times with the same bunching factor for high harmonics.

4 Hard X-rays based on cascaded PEHG scheme

The parameters of the electron beams, undulators and seed laser system were summarized in the last section. Here, we give details of the FEL operation. The

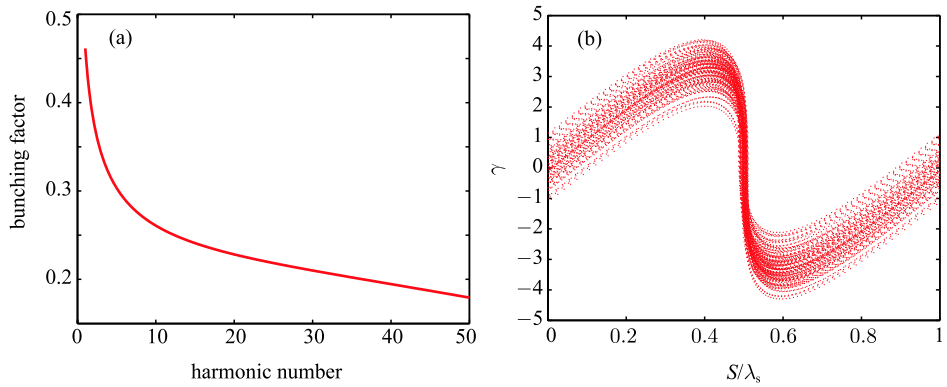

Fig. 2. (a) PEHG bunching factor evolution for energy modulation amplitude $A = 5$; (b) PEHG phase space after passing through DS1, where S/λ_s is the ratio of e-beam coordinate to seed laser wavelength.

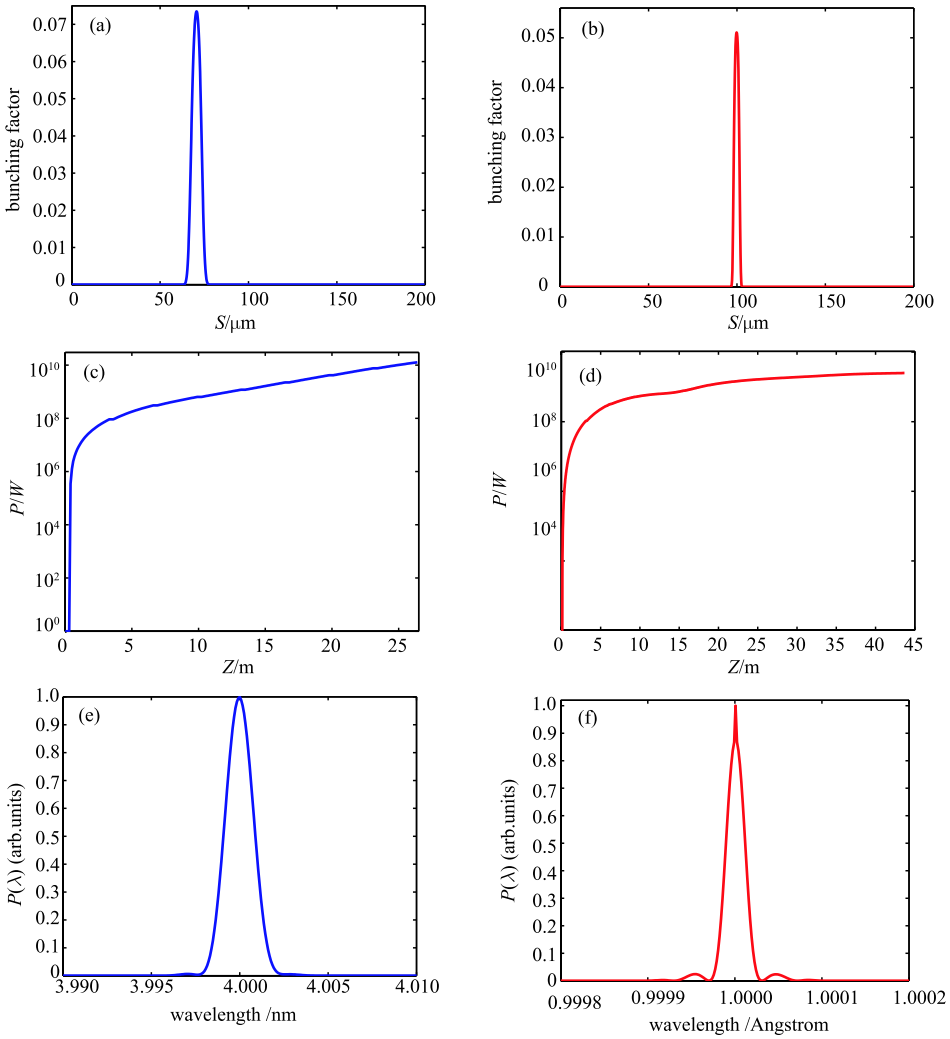

Fig. 3. FEL performances in two stages. (a) 50th harmonic bunching factor distribution along the electron beam coordinate (S/μm) at the entrance of the radiator in the first stage; (b) 40th harmonic bunching factor distribution along the electron beam at the entrance of the radiator in the second stage; (c) output radiation peak power along the undulator coordinate (Z/m) of the first stage; (d) output radiation peak power of the second stage; (e) spectrum of the radiation generated by the first stage; and (f) spectrum of the radiation generated by the second stage.

first stage of the cascaded PEHG is expected to generate 4 nm FEL radiation from the 200 nm seed laser with longitudinal Gaussian profile and 10 GW peak power. The FWHM length of the seed laser pulse is about 50 fs, which is much shorter than the designed electron bunch length. Only a fraction of the beam is modulated in M1 and produces coherent radiation in R1. The radiation will be shifted to a fresh part of the electron by the shifter and severs as the seed laser for the second stage. A drift is located after the first stage for lattice matching and diffusion of the FEL radiation from first stage. A modulator system consisting of a normal planar undulator and a TGU is proposed for the second stage PEHG. According to Ref. [18], for a relatively small energy modulation, this configuration enables nearly the same bunching factor compared with the first stage layout. This reduces the power requirements for the first radiator and improves the output performances of the cascaded PEHG scheme. Finally, the 1 Å radiation will be generated by the modulated fresh bunch in R2.

On the basis of the parameters shown in Table 1, time dependent simulation has been carried out to assess the FEL lasing results by the well-benchmarked FEL code GENESIS [31]. To obtain realistic simulation results, the whole electron beam was tracked through the first stage to the second stage PEHG. The simulation results are shown in Fig. 3. In view of the tradeoff between the seed laser induced energy spread and the available bunching factor, a moderate energy modulation amplitude of $A_1 = 5$ is chosen for FEL gain process in the M1, then the e-beam is well bunched after the DS1, and the bunching factor of 50^{th} harmonic is optimized to 7% at the entrance of the first radiator. The 4 nm FEL radiation pulse is generated with output power of 5 GW and the pulse length of the seed laser is also maintained. A matching section is located after the first stage in order to provide adjustable beta-matching, diffusion of FEL spot and smear out the e-beam micro-bunching generated in the first stage. The energy modulation amplitude for the second stage is $A_2 = 5$ and the 40^{th} harmonic bunching factor is optimized to be 5%(Fig. 3 (b)) The FEL radiation generated by the fresh part saturates after 40 m with a peak power of 2 GW. After passing through the 40 m long radiator, the relative FWHM bandwidth of the 1 Å radiation is about 4×10^{-5} and close to Fourier transform limited. The spectral emission presents a regular quasi-perfect Gaussian shape pulse-to-pulse, with little redshift compared with 1 Å radiation, due to the energy loss of the e-beam in the lasing process. The noisy spike and slight FEL spectrum broadening are induced mainly by the amplification of intrinsic shot noise in the e-beam, which is proportional to the harmonic number h. Moreover, the FEL peak power in Fig. 3 (b) and (d) increases continuously, because the main FEL pulse slips to the unsaturated electron beam in the radiator.

5 Dogleg design for the cascaded PEHG beam line

The PEHG mechanism requires a large dogleg to provide the R_{16} used for transverse dispersion of the e-beam. This necessary dispersion will lead to increased beam size and transverse emittance, which will definitely degrade the PEHG performance. Thus, we concentrate on the effects of the dispersion dogleg in the e-beam in this section. Two dipole doglegs are widely used to translate the beam axis horizontally or vertically. Quadrupoles are placed between the two consecutive dipoles to match first-order dispersion and provide beta focusing. The transform matrix of a dogleg can be described as Eq. (4), where L is the length of drift space, θ and ρ is the bend angle and bend radius, respectively.

$$\begin{vmatrix} 1+\frac{L}{\rho}\cos\theta\sin\theta & L\cos^2\theta & 0 & 0 & 0 & -L\cos\theta\sin\theta \\ \frac{L}{\rho^2}\sin^2\theta & 1-\frac{L}{\rho}\cos\theta\sin\theta & 0 & 0 & 0 & \frac{L}{\rho}\sin^2\theta \\ 0 & 0 & 1 & L & 0 & 0 \\ 0 & 0 & 0 & 1 & 0 & 0 \\ -\frac{L}{\rho}\sin^2\theta & -L\cos\theta\sin\theta & 0 & 0 & 1 & L\sin^2\theta \\ 0 & 0 & 0 & 0 & 0 & 1 \end{vmatrix} \tag{4}$$

The dispersion strength of a dogleg can be estimated as $\eta = -L\cos\theta\sin\theta$, and as mentioned, η is about 1.4m for the cascaded PEHG scheme to generate sufficient transverse off-set in the e-beam. In this section, we design two different doglegs to compare the effects of transverse dispersion in the e-beam The corresponding bend angle of this dogleg is designed as 3°. A so-called π insertion composed of quadrupoles will be placed between the bending magnets to cancel the effects of the elements placed on either side of them For an achromatic dogleg, the same configuration is utilized for comparison. The beta function at the exit of the two schemes

is nearly the same, both being about 25 m. ELEGANT is used for the simulation of beam evolution in the dogleg [32]. Figure 4 shows the e-beam transverse phase space distribution after the dogleg. Due to the dispersion, an obvious energy chirp happened along the σ_x coordinate of the e-beam. This artificial energy chirp is adjustable to match the transverse gradient of the TGU magnet field. The beam size is increased about 3 times for the dispersion dogleg. Furthermore, the dispersion terms will introduce a transverse position jitter related to the e-beam energy jitter, so a large seed laser transverse spot size is required to cover the whole e-beam, which means that a high pulse energy seed laser is needed.

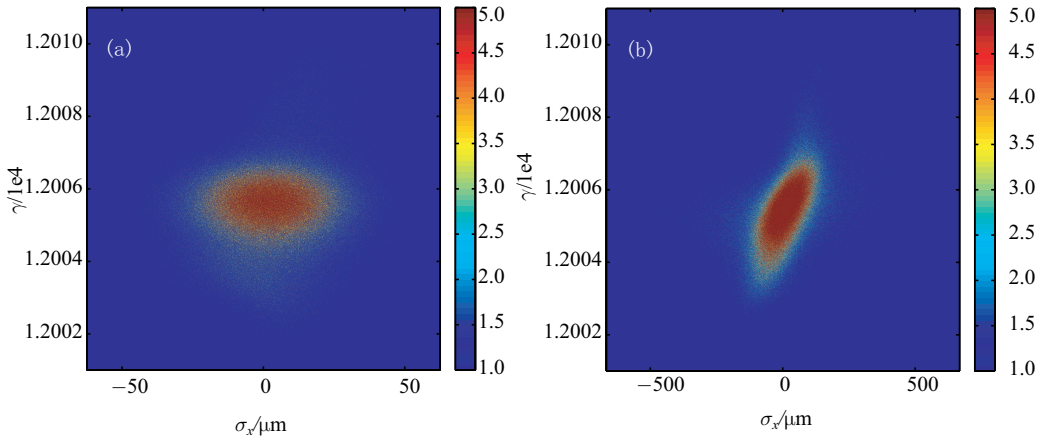

Fig. 4. e-beam phase space distribution after achromatic dogleg (a) and dispersive dogleg (b). The bend angle of the dogleg is 3° and the total length is about 29 m.

Figure 5(a), (b) show the lattice and dispersion evolution along the dogleg coordinate. The beta function at the exit is nearly the same, both about 25 m, to optimize the beam size after the transport process; the corresponding dispersion is summarized in Fig. 5(b), and the parameter η can be effectively controlled by the π insertion Figure 5 (c) and (d) show the simulation results of the e-beam at the exit of the dogleg. Due to the increase of transverse beam size in the x-direction, the transverse emittance is almost doubled compared with the achromatic case. Benefitting from the small deflection angle, the effects of coherent synchrotron radiation (CSR) in emittance increase can be ignored in our case. The emittance increase will definitely degrade the PEHG bunching performance, but this can be compensated with large energy modulation amplitude [17–18]. In Fig. 5 (c), due to the wake field and un-vanished R_{56} terms, a little increase of bunch length can be observed. The double horn distribution is mainly induced by x-z coupling in the e-beam and the statistical methods of ELEGANT itself. As mentioned above, the dogleg is horizontal, and the beam quality in the y-direction can be perfectly preserved. Finally, it is worth emphasizing that the beam tracking in this section is based on an ideal e-beam. More detailed issues, such as the effects of strong CSR in the dipole, beam lattice evolution in the undulator system and effects of beam distribution along the time coordinate should be further studied.

6 Conclusion

Design studies for a cascaded PEHG scheme for potential hard X-ray FEL projects are presented. Compared with the cascaded HGHG, only two stages of PEHG are needed to reach the hard X-ray region in this scheme. Due to the living doglegs in multi-branch FEL facilities, the cascaded PEHG is simple in layout and has easier laser-beam synchronization and better FEL spectrum in real operation than the cascaded EEHG. The results here show that using the realistic beam parameters, 0.1 nm coherent hard X-ray FEL with peak power up to 2 GW can be generated directly from a 200 nm seed laser based on this scheme. Some practical limiting factors that might affect the performance of cascaded PEHG scheme are also taken into account. According to the simulations, it is also found that the dogleg will introduce an increase of the horizontal beam size, and it is necessary to utilize a powerful seed laser to modulate the e-beam. These requirements can be totally fulfilled by state-of-the-art laser technology. Further more detailed studies, including of the CSR in the bending magnet, e-beam lattice in the undulator system and the effects of the longitudinal beam distribution, still need to be analyzed in the future.

The authors are grateful to Bo Liu, Guorong Wu, Dong Wang and Zhentang Zhao for helpful discussions.

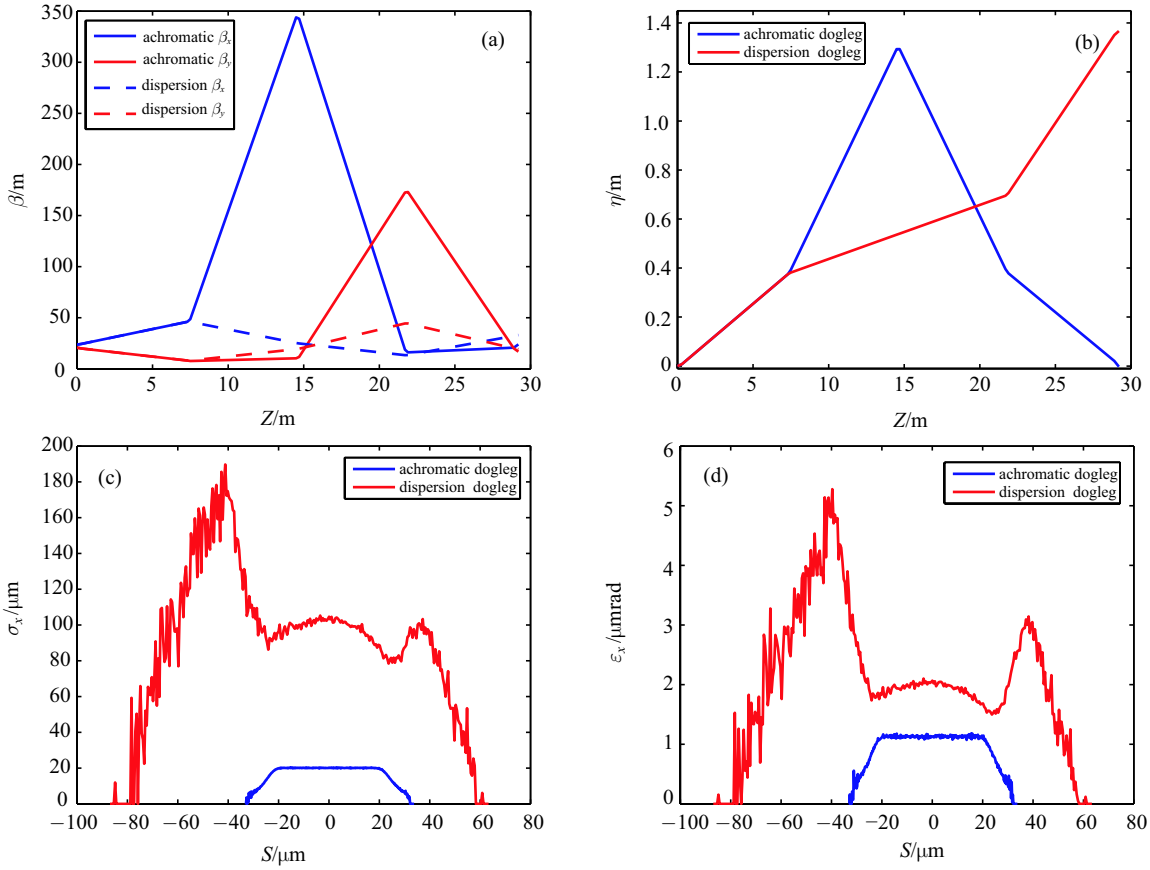

Fig. 5. (color online) Beta function (a) and dispersion evolution (b) along the dogleg coordinate (Z/m); transverse e-beam size in x-direction (c) and emittance growth due to the dispersion of dogleg (d), with (red) and without dispersion (blue).

References

1 Emma P. et al, Nature Photon **4:** 641-647 (2010)
2 E. Allaria et al, Nature Photon, **6:** 699-704 (2012)
3 http://flash2.desy.de/
4 Concept Design Report, Soft X-ray Free Electron Laser Test Facility, Shanghai, May 2015
5 Deng, H. et al, Chin. Phys. C, **38:** 028101 (2014)
6 L. H. Yu, Phys. Rev. A, **44:** 5178 (1991)
7 L. H. Yu et al, Science, **289:** 932-934 (2000)
8 L. H. Yu et al, Phys. Rev. Lett., **91:** 074801 (2003)
9 M Labat et al, Phys. Rev. Lett., **107:** 224801 (2011)
10 G. Stupakov, Phys. Rev. Lett., **102:** 074801 (2009)
11 D. Xiang and G. Stupakov, Phys. Rev. ST Accel. Beams, **12:** 030702 (2009)
12 D. Xiang et al, Phys. Rev. Lett., **105:** 114801 (2010).
13 Z. T. Zhao, D. Wang et al, Nature Photon, **6:** 360-363 (2012)
14 E.L. Saldin et al, Opt. Commun., **202**: 169-187 (2002)
15 Wu J H et al, Nucl. Instrum. Methods Phys. Res., Sect. A, **475:** 104-111 (2001)
16 C. Feng et al, Chin. Sci. Bull., **55:** 221-227 (2010)
17 H. X. Deng and C. Feng, Phys. Rev. Lett., **111:** 084801 (2013)
18 C. Feng, H. Deng, D. Wang, and Z. Zhao, New J. Phys., **16:** 043021 (2014)
19 T. I. Smith et al, Journal of Applied Physics, **50:** 4580 (1979)
20 G. Wang et al, Nucl. Instrum. Methods Phys. Res., Sect. A, **753:** 56-60 (2014)
21 J. H. Han et al, TUPPP061, in *Proceedings of IPAC2012*, New Orleans, Louisiana, USA
22 Makina Yabashi et al, J. Synchrotron Rad., **22:** 477-484 (2015)
23 SWISS-FEL Concept Design Report
24 Yu L H and Ben-Zvi I, Nucl. Instrum. Methods Phys. Res., Sect. A, **393:** 96-99 (1997)
25 Deng H X and Dai Z M, Chin. Phys. C, **32:** 236-242 (2008)
26 Feng C et al, Chin. Sci. Bull., **57:** 3423-3429 (2012)
27 B. Liu et al, Phys. Rev. ST Accel. Beams, **16:** 020704 (2013)
28 E. Allaria et al, Nature Photonics, **7:** 913-918 (2013)
29 Coisson R and MartiniF D, Phys Quant Electron, **9:** 939960 (1982)
30 Goloviznin V and Amersfoort P W, Phys. Rev. E, **55:** 60026010 (1997)
31 S. Reiche, Nucl. Instrum. Methods A, **429:** 243-248 (1999)
32 M. Borland, ANL Advanced Photon Source, Report No. LS-287, 2000